miR-30e-5p attenuates neuronal deficit and inflammation of rats with intracerebral hemorrhage by regulating TLR4

HAIPENG SONG[1], NA XU[2] and SHAN JIN[3]

Departments of [1]Neurosurgery and [2]Emergency, Jinan First People's Hospital, Ji'nan, Shandong 250012; [3]Department of Neurology, The 960th Hospital of The Chinese People's Liberation Army, Ji'nan, Shandong 250031, P.R. China

Received January 20, 2022; Accepted April 7, 2022

DOI: 10.3892/etm.2022.11419

Abstract. microRNAs (miRNAs or miRs) have been reported to regulate the pathology of intracerebral hemorrhage (ICH). Therefore, the present study aimed to investigate the function of miR-30e-5p in rats with ICH with specific focus on Toll-like receptor (TLR)4. In the present study, collagenase type IV was used for the establishment of the ICH model in rats, prior to which the rats were injected with miR-30e-5p mimic or miR-30e-5p mimic + pcDNA3.1-TLR4 plasmid. The expression levels of miR-30e-5p and TLR4 were then measured using reverse transcription-quantitative PCR and western blotting. The potential interaction between miR-30e-5p and TLR4 was tested using the MicroRNA Target Prediction Database and dual-luciferase reporter and RNA immunoprecipitation assay. In addition, the concentration of TNF-α, IL-6 and IL-1β was measured using ELISA. The protein expression levels of TLR4/myeloid differentiation factor 88 (MyD88)/TIR-domain-containing adapter-inducing interferon-β (TRIF) signaling-associated molecules were measured by western blotting. Following induction of ICH, miR-30e-5p expression was downregulated, while TLR4 expression was upregulated. By contrast, injection with miR-30e-5p mimic rescued neuronal function while suppressing neuronal inflammation in rats following ICH; these effects were reversed by co-overexpression of TLR4. Furthermore, overexpression of miR-30e-5p inactivated TLR4/MyD88/TRIF signaling in rats with ICH; this was also reversed by overexpression of TLR4. Taken together, these results suggested that overexpression of miR-30e-5p exerted a protective role against neuronal deficit and inflammation caused by ICH in rats by targeting TLR4 and inactivating TLR4/MyD88/TRIF signaling.

Correspondence to: Dr Shan Jin, Department of Neurology, The 960th Hospital of The Chinese People's Liberation Army, 25 Shifan Road, Ji'nan, Shandong 250031, P.R. China
E-mail: jinshanla@126.com

Key words: intracerebral hemorrhage, neuronal function, inflammation, microRNA-30e-5p, Toll-like receptor

Introduction

Intracerebral hemorrhage (ICH) is a type of stroke that is relatively common but lacks clear treatment strategy (1). ICH accounts for 10-15% of all cases of stroke in the US (2). In Globally, ICH is one of the most deleterious types of all strokes; it has an incidence of 10-30 per 100,000 patients annually, with a morbidity rate of 75% and a mortality rate of 30-50% January 1980, and November 2008 (3). ICH is diagnosed more frequently in the elderly (>55 years old) and in males, with predilection observed in patients of African and Asian ethnicity (4,5). Hematoma following ICH destroys the surrounding vascular system, which induces hemorrhage and potentiates growth of hematoma, which leads to neuronal deficit (6). Furthermore, ICH induces inflammation to promote edema formation, which aggravates the hydrostatic pressure around the hematoma, resulting in cell death (7,8).

Neurological deficit, which is typically caused by neuroinflammation, is associated with the release of endogenous ligands that primarily activate Toll-like receptors (TLRs) (9). Accumulating evidence suggests that TLR4-mediated neuroinflammation is one of the key causes of secondary brain injury following ICH (10,11). Upregulated TLR4 expression levels are associated poorer outcomes in patients with ICH (12). By contrast, treatment with antagonists of TLR4 attenuates brain injury following ICH (13).

microRNAs (miRNAs or miRs) belong to a family of small non-coding RNAs that are ~20 nucleotides in length (14). They regulate expression of target mRNAs, in turn regulating a number of human diseases (14-17). Numerous miRNAs have been documented as potential molecular markers for diagnosis, treatment and development of ICH (15), including miR-183-5p (16) and miR-331-3p (17). According to results from a miRNA PCR array, miR-30e-5p expression is downregulated in peripheral blood samples from patients with ICH (18). However, little is known about the role of miR-30e-5p in ICH.

A number of studies have reported the effect of miR-30e-5p in human disease, such as squamous cell carcinoma of the head and neck, where it inhibits metastasis and angiogenesis by targeting astrocyte elevated gene-1 expression (19,20). Furthermore, miR-30e-5p has been found to reverse hypoxia-induced apoptosis of human stem cell-derived

cardiomyocytes by targeting Bim expression (21). A previous study observed that miR-30e-5p suppresses inflammation and protects against cardiac dysfunction following myocardial infarction by targeting PTEN expression (22). Nevertheless, the potential association between miR-30e-5p and TLR4, in addition to their physiological roles in ICH remain poorly understood. Therefore, the present study investigated the effect of miR-30e-5p overexpression on neuronal function and apoptosis and inflammation, in addition to TLR4 signaling, in rats with ICH.

Materials and methods

Animals. Healthy male adult Sprague-Dawley rats (n=72; age, 10-12 weeks; weight, 250-300 g; Model Animal Research Center of Nanjing University) were maintained at 22-25˚C with 12/12-h day/night cycle, humidity of 50-60% and free access to food and water at specific-pathogen-free grade. The animal experiments were approved by the Institutional Animal Care and Use Committee of Jinan First People's Hospital (approval no. JNFPH2019-03; Ji'nan, China). The total duration of the experiment was 10 days from the establishment of animal models to complete assessment of the neurological function. After collecting blood in tail vein, rats were anesthetized with intraperitoneal injection of 3% pentobarbital sodium (30 mg/kg) and sacrificed by cervical dislocation. Death was confirmed by cessation of breathing and faded eye color.

Groups. miR-negative control (NC) mimic, miR-30e-5p mimic, pcDNA3.1, and pcDNA3.1-TLR4 were purchased from Shanghai GenePharma Co., Ltd. Rat is an ideal pathophysiological disease model that is widely used (23,24). The ICH model in rats was established by IC injection of collagenase type IV (0.23 U in 1 μl sterile saline; Beijing Solarbio Science & Technology Co., Ltd.) into the right striatum, as previously described (25). For the rats in the ICH group (n=11), miR-NC mimic + pcDNA3.1 was injected into the right lateral ventricle of rats 3 days prior to the establishment of ICH model.

Rats in the sham group (n=11) were injected with 1 μl sterile saline. For rats in the remaining groups (ICH + miR-30e-5p mimic + pcDNA3.1 and ICH + miR-30e-5p mimic + pcDNA3.1-TLR4; both n=11), miR-30e-5p mimic + pcDNA3.1 or miR-30e-5p mimic + pcDNA3.1-TLR4 was injected into the right lateral ventricle of rats 3 days prior to establishment of ICH model (26).

Neurological function. A 24-point neurological scoring system was used to test neurological deficit, including Longa, beam balance test (BBT), Bederson and foot fault asymmetry in rats. Neurological function was assessed on day 7 after the establishment of ICH. Longa standards (27) were as follows: 0, no neurological impairment; 1, impaired stretching of contralateral limbs; 2, circling around; 3, tilting to the side of hemiplegia upon waking and 4, impaired walking or unconsciousness.

The rats underwent BBT, in which they were allowed to walk on a balance beam (square stick; length, 80.0 cm; width, 2.5 cm; 10.0 cm above ground) to walk on. The following six-grade standard was applied (28): 0, jump on the balance beam and walk without falling; 1, jump on the balance beam with time of falling ≤50%; 2, jump on the balance beam with time of falling >50%; 3, jump on the balance beam with the healthy lateral hind limb with no movement of paralyzed hind limb; 4, sit on the balance beam without walking and 5, fall from the balance beam.

For Bederson score which is used for disability assessment (29), the rats were lifted 10 cm above the desk. After seizing the tail by an experimenter, healthy rats should straighten the foreleg. The standards used for scoring this were as follows (29): 0, no neurological impairment; 1, lateral wrist and elbow joint flexion and shoulder adduction and flexion; 2, lateral wrist and elbow joint flexion, shoulder adduction and flexion and decreased thrust to the paralytic side and 3, chasing tail with circling to the paralytic side.

For foot fault asymmetry score, rats were placed in a wet box (2.3x2.3 cm mesh) and the number of times the forelegs touched the mesh was counted. Score was calculated as follows (30): (no. of missteps of forelegs opposite to the lesion-no. of missteps of forelegs on the same side as the lesion)/total steps. A positive score indicates impaired function toward the lesion, while a negative score indicates impairment of function on the same side as the lesion.

ELISA. Following the measurement of neurological deficit in rats, 1 ml blood from the tail vein was collected and centrifuged at 1,500 x g for 10 min at 4˚C. Serum samples were stored at -20˚C. The concentration of IL-6 (cat. no. ERA31RBX10), TNF-α (cat. no. ERA56RB) and IL-1β (cat. no.# BMS630TEN) was evaluated using ELISA kits (all Thermo Fisher Scientific, Inc.) according to the manufacturer's protocols. Optical density was measured at 450 nm using a BioTek Epoch microplate reader.

Reverse transcription-quantitative (RT-q)PCR. TRIzol® (Invitrogen; Thermo Fisher Scientific, Inc.) was used to extract total RNA from rat brain tissue. RNA (1 μg) was subjected to RT using avian myeloblastosis virus reverse transcriptase (Takara Biotechnology Co., Ltd.) following manufacturer's protocol. The quantification of cDNA was performed using SYBR Premix Ex Taq™ (Takara Biotechnology Co., Ltd.) and LightCycler 480 system (Roche Diagnostics). The thermocycling conditions were as follows: Initial denaturation at 95˚C for 10 min, followed by 40 cycles of 95˚C for 10 sec, 60˚C for 20 sec and 72˚C for 10 sec. U6 was used as the internal reference for miR-30e-5p, while GAPDH was used as the internal reference for TLR4. The primer sequences are listed in Table I. The gene expression was analyzed by the $2^{-\Delta\Delta Cq}$ method (31).

Western blotting. Total protein from brain tissue of rats was extracted using RIPA buffer (Roche Diagnostics). Protein concentration was using BCA kit (Boster Biological Technology). In total, 30 μg protein sample was loaded into each lane, followed by separation by 8% SDS-PAGE. Next, proteins were transferred onto PVDF membranes, followed by blocking with 5% BSA (Thermo Fisher Scientific, Inc.) for 1 h at room temperature and incubation with primary antibodies against TLR4 (1:1,000; cat. no. 19811-1-AP; Proteintech Group, Inc.), GAPDH (1:2,500; cat. no. ab9485; Abcam), myeloid differentiation factor 88 (MyD88; 1:1,000; cat. no. ab2064; Abcam) and TIR-domain-containing adapter-inducing IFN-β

Table I. Primer sequences for reverse transcription-quantitative PCR.

Name	Forward	Reverse
GAPDH	5'-CCATAAAGGGCATCCTGGGCT-3'	5'-TTACTCCTTGGAGGCCATGTA-3'
U6	5'-CTCGCTTCGGCAGCACA-3'	5'-AACGCTTCACGAATTTGCGT-3'
miR-30e-5p	5'-TGTAAACATCCTTGACTGGAAG-3'	5'-CTTCCAGTCAAGGATGTTTACA-3'
TLR4	5'-CGCCTAAAACCCATTATGTTTACA-3'	5'-TGTAAACATAATGGGTTTTAGGCG-3'

miR, microRNA; TLR, Toll-like receptor.

(TRIF; 1:1,000; cat. no. ab13810; Abcam) overnight at 4˚C. The membranes were rinsed using 0.1% TBST three times for 5 min each, before being incubated with horseradish peroxidase-conjugated anti-rabbit IgG secondary antibody (1:5,000; cat. no. ab288151; Abcam) for 1 h at room temperature. The membranes were rinsed using 0.1% TBST three times for 5 min each and developed using Pierce enhanced chemiluminescence system (Thermo Fisher Scientific, Inc.). GAPDH was used as the internal reference. Image J (Version 1.8.0, National Institutes of Health) was used for the analysis of the gray value.

Cell culture. PC12 cells were purchased from the American Type Culture Collection and maintained in DMEM supplemented with 10% FBS and 1% penicillin-streptomycin (all Invitrogen; Thermo Fisher Scientific, Inc.) at 37˚C with 5% CO_2.

Dual luciferase reporter assay. The potential interaction between TLR4 and miR-30e-5p was predicted using MicroRNA Target Prediction Database (mirdb.org). Rat wild-type TLR4 3'-untranslated region (UTR), which contained potential binding sites for miR-30e-5p, was cloned into the pmirGLO vector (Promega Corporation). Mutant TLR4 3'-UTR was obtained using Q5 Site-Directed Mutagenesis kit (cat. no. E0554S; New England BioLabs, Inc.) according to the manufacturer's protocol.

PC12 cells ($2x10^5$) were seeded in 6-well plates and co-transfected with wild-type or mutant TLR4 luciferase construct alongside mimic negative control (NC) (5'-UUC UCCGAACGUGUCACGU-3') or miR-30e-5p mimic (5'-UGU AAACAUCCUUGACUGGAAG-3') for 48 h at 37˚C using Lipofectamine® 2000 (Invitrogen; Thermo Fisher Scientific, Inc.) according to the manufacturer's protocol. At 48 h after transfection, luciferase activity was evaluated using the Dual-Luciferase Reporter Assay System (Promega Corporation) and normalized to that of the *Renilla* construct.

RNA immunoprecipitation (RIP) assay. Firstly, nuclei were extracted using NP-40 lysis buffer (240 μl, Beyotime Institute of Biotechnology) from PC12 cells ($5x10^6$) by centrifugation at 15,000 x g and 4˚C for 10 min, lysed and incubated with primary antibodies against argonaute2 (Ago2; 1: 30, 8 μl; cat. no. ab186733; Abcam) and negative control IgG (1:30 (8 μl); cat. no. ab205718; Abcam) at 4˚C overnight. RNA immunoprecipitated with Ago2 was isolated following addition of 25 μl protein A agarose (cat. no. ab169993; Abcam) and protein G agarose beads (cat. no. ab174816; Abcam) following manufacturer's protocol. Completes were isolated by centrifugation at 1,000 x g for 5 min at 4˚C and boiling for 3 min. After washing with ice cold low salt wash buffer, RNA was purified and reverse-transcribed into cDNA. Gene expression was assessed by RT-qPCR, as aforementioned.

Statistical analysis. Data analysis was performed using SPSS 21.0 (IBM Corp.). All experiments were repeated three times. All data are presented as mean ± standard deviation. Unpaired t-test was used for comparisons between two groups, while one-way analysis of variance followed by Tukey's post hoc test was used for comparisons between >2 groups. The correlation between miR-30e-5p and TLR4 was assessed by Pearson's correlation analysis. $P<0.05$ was considered to indicate a statistically significant difference.

Results

Verification of establishment of ICH in rats. First, successful establishment of ICH in rats was determined. The neurological function scores of rats in the ICH group, including those of Longa (Fig. 1A), BBT (Fig. 1B), Bederson (Fig. 1C) and foot fault asymmetry (Fig. 1D), were significantly higher compared with those in the sham group, indicating successful establishment of ICH in rats.

miR-30e-5p expression is decreased and TLR4 expression is increased following ICH. TLR4 mRNA expression levels were significantly upregulated in the perihematomal striatum of rats at 24 h following ICH compared with the sham group (Fig. 2A). To identify the potential role of miR-30e-5p following ICH, miR-30e-5p expression was measured in the perihematomal striatum from rats with ICH. miR-30e-5p expression was lower in the perihematomal striatum of rats at 24 h following ICH compared with the sham group (Fig. 2B). In addition, there was an inverse correlation between TLR4 and miR-30e-5p expression in the perihematomal striatum of rats at 24 h following ICH (Fig. 2C). Moreover, TLR4 protein expression levels (Fig. 2D and E) were upregulated in the perihematomal striatum of rats at 24 h following ICH compared with those in the sham group. The findings indicated the opposite roles of miR-30e-5p and TLR4 in ICH.

TLR4 is a direct target of miR-30e-5p in PC12 cells. The potential association between miR-30e-5p and TLR4 was predicted by sequence complementarity according to miRDB

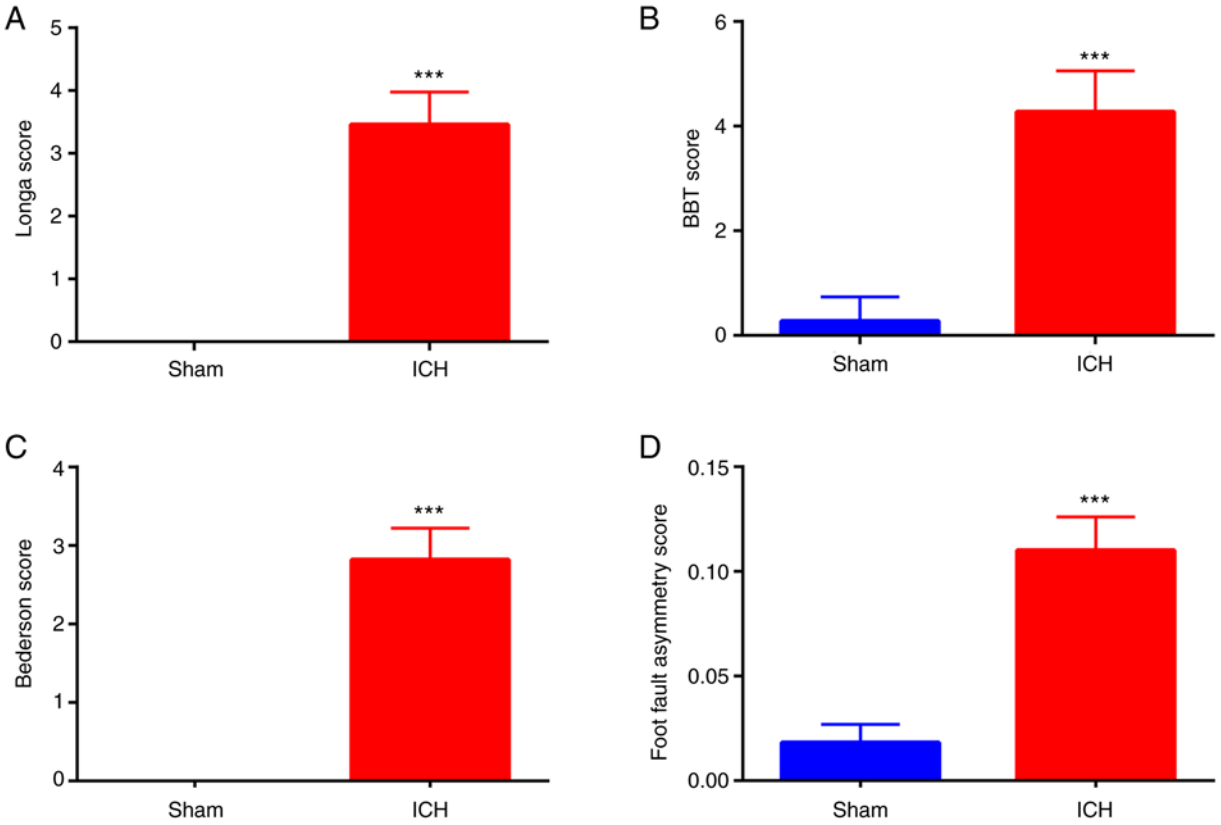

Figure 1. Establishment of ICH in rats. Neurological function was determined by (A) Longa, (B) BBT, (C) Bederson and (D) foot fault asymmetry score in sham and ICH group. n=11. ***P<0.001 vs. sham. ICH, intracerebral hemorrhage; BBT, beam balance test.

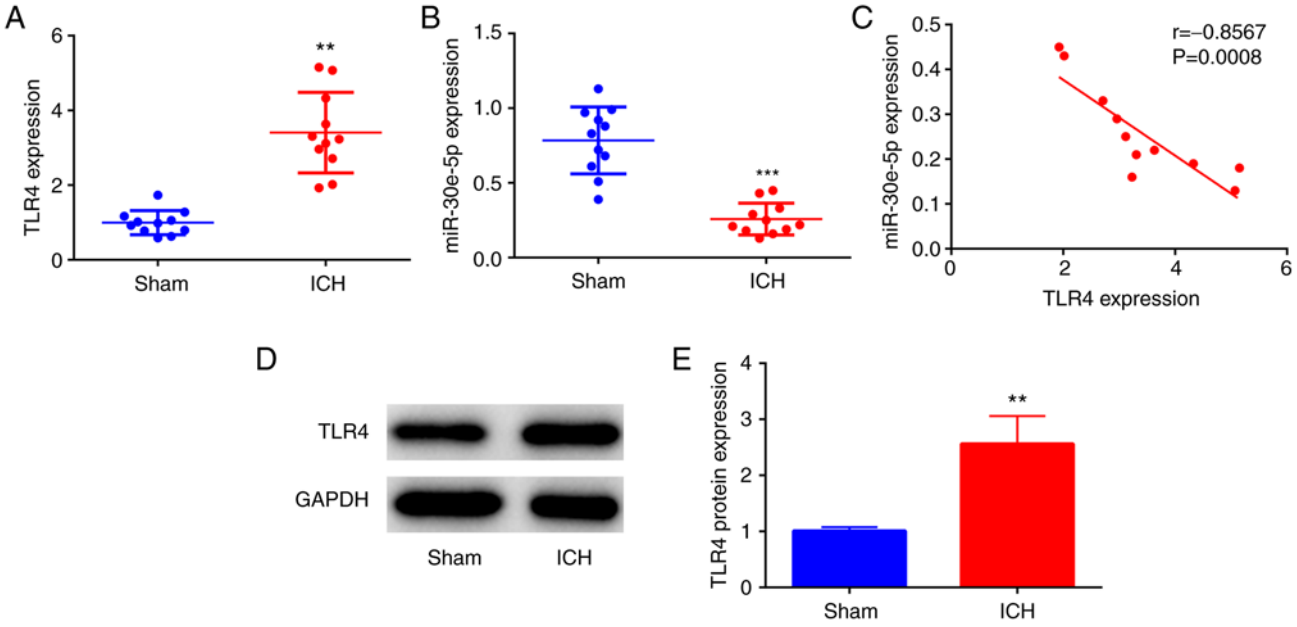

Figure 2. miR-30e-5p is decreased and TLR4 is increased following ICH. Reverse transcription-quantitative PCR was used to detect (A) miR-30e-5p and (B) TLR4 expression in sham and ICH group. (C) Pearson's correlation analysis was used to analyze the correlation between miR-30e-5p and TLR4 in ICH group (n=11). (D) Western blot analysis was used to detect (E) TLR4 protein expression levels in sham and ICH group (n=3). **P<0.01, ***P<0.001 vs. sham. miR, microRNA; TLR, Toll-like receptor; ICH, intracerebral hemorrhage.

(Fig. 3A). To verify if miR-30e-5p directly targets the 3'-UTR of TLR4, dual luciferase reporter assay was performed in PC12 cells. miR-30e-5p mimic was effectively transfected into PC12 cells, as evidenced by upregulated expression levels of miR-30e-5p in the miR-30e-5p mimic compared with miR-NC mimic group (Fig. 3B). In addition, compared with miR-NC mimic, miR-30e-5p mimic inhibited luciferase activity of wild-type TLR4 3'-UTR construct but not that of

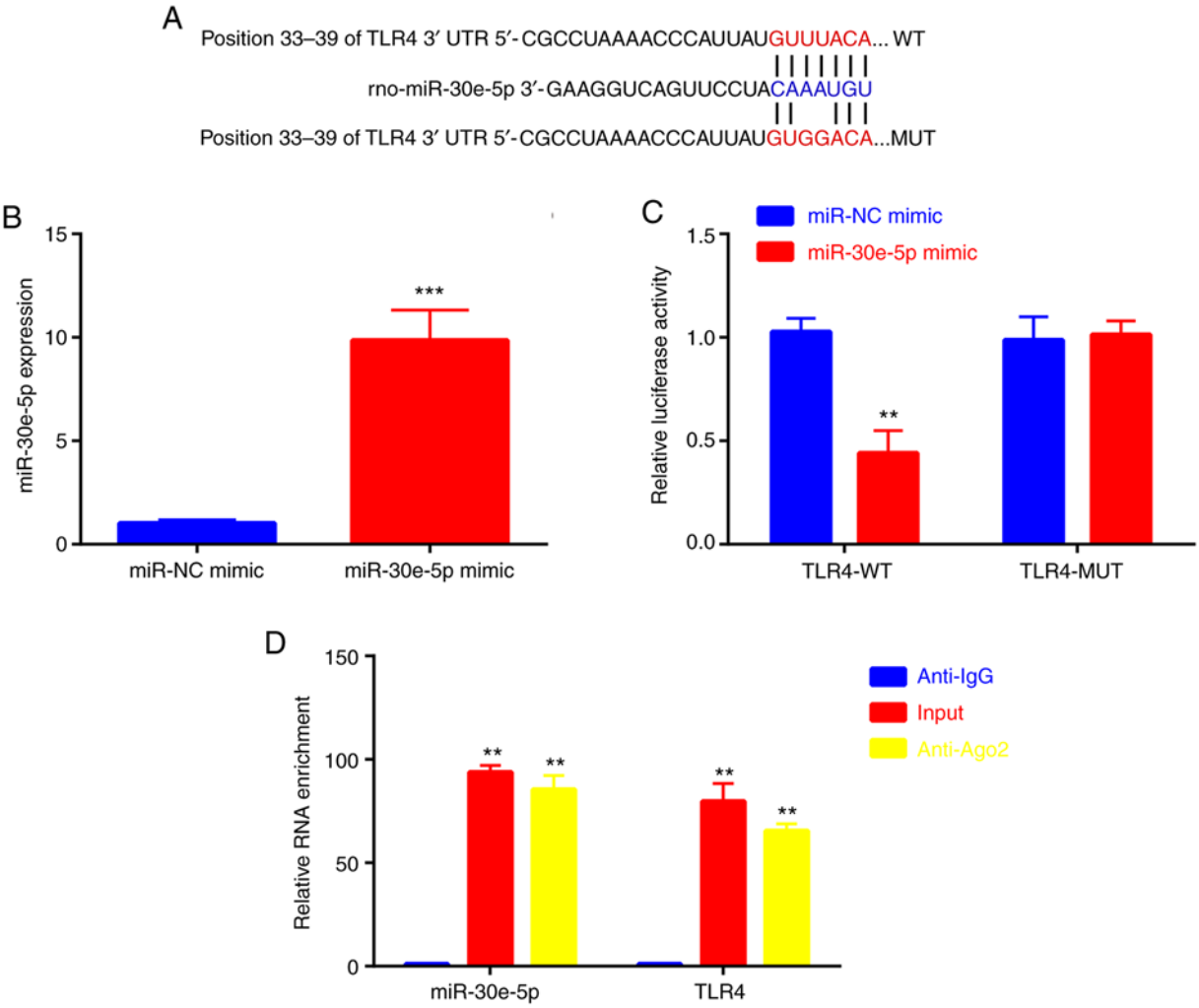

Figure 3. TLR4 is a direct target of miR-30e-5p in PC12 cells. (A) Association between miR-30e-5p and TLR4 was predicted by MicroRNA Target Prediction Database. (B) Reverse transcription-quantitative PCR analysis was used to detect miR-30e-5p levels in miR-NC and miR-30e-5p mimic groups. (C) Dual luciferase reporter assay was used to test luciferase activity. **P<0.01, ***P<0.001 vs. miR-NC mimic. (D) RIP assay was used to detect miR-30e-5p and TLR4 enrichment in Anti-IgG, Input, and Anti-Ago2 group. n=3. **P<0.01 vs. Anti-IgG. miR, microRNA; TLR, Toll-like receptor; NC, negative control; Ago2, argonaute2; UTR, untranslated region; WT, wild-type; MUT, mutant.

the mutant construct (Fig. 3C). The RIP assay showed that IgG did not enrich miR-30e-5p or Ago2 compared with input, indicating the success of RIP assay. RIP assay revealed that both miR-30e-5p and TLR4 were significantly enriched in the Ago2 group (Fig. 3D), suggesting that miR-30e-5p directly targets the 3'UTR of TLR4 in PC12 cells.

miR-30e-5p overexpression attenuates neurological deficit and inflammation by targeting TLR4 following ICH. To clarify the association between miR-30e-5p and TLR4 in ICH, miR-30e-5p and TLR4 was overexpressed by IC ventricular injection of miR-30e-5p mimic and pcDNA3.1-TLR4 3 days prior to establishment of ICH in rats. miR-30e-5p was successfully overexpressed in the perihematomal striatum of rats, which was reflected by significantly increased miR-30e-5p expression levels compared with those injected with miR-NC mimic (Fig. 4A). pcDNA3.1-TLR4 was successfully transfected into the perihematomal striatum of rats, which was shown by increased TLR4 expression compared with that in the pcDNA3.1 group (Fig. 4B). The neurological deficit of rats with ICH, including Longa (Fig. 4C), BBT (Fig. 4D), Bederson (Fig. 4E) and foot fault asymmetry (Fig. 4F) was alleviated by overexpression of miR-30e-5p; this effect was reversed by co-overexpression of TLR4. Additionally, serum levels of proinflammatory cytokines TNF-α, IL-1β, and IL-6 in rats were decreased by overexpression of miR-30e-5p; this was reversed by co-overexpression of TLR4 (Fig. 5A-C). The findings indicated the opposite roles of miR-30e-5p and TLR4 in neurological deficit and inflammation.

miR-30e-5p overexpression suppresses TLR4 expression and inactivates downstream MyD88/TRIF signaling following ICH. To determine whether the neuroprotective role of miR-30e-5p in rats with ICH was associated with regulation of TLR4 and MyD88/TRIF signaling, the expression profile of associated proteins was assessed in the perihematomal striatum of rats. miR-30e-5p overexpression decreased TLR4 expression levels as well as those of MyD88 and TRIF, which were originally induced by ICH. However, the inhibitory effects of miR-30e-5p overexpression were partially reversed by co-overexpression of TLR4 (Fig. 6A and B). The findings indicated the opposite roles of miR-30e-5p and TLR4 in MyD88/TRIF signaling.

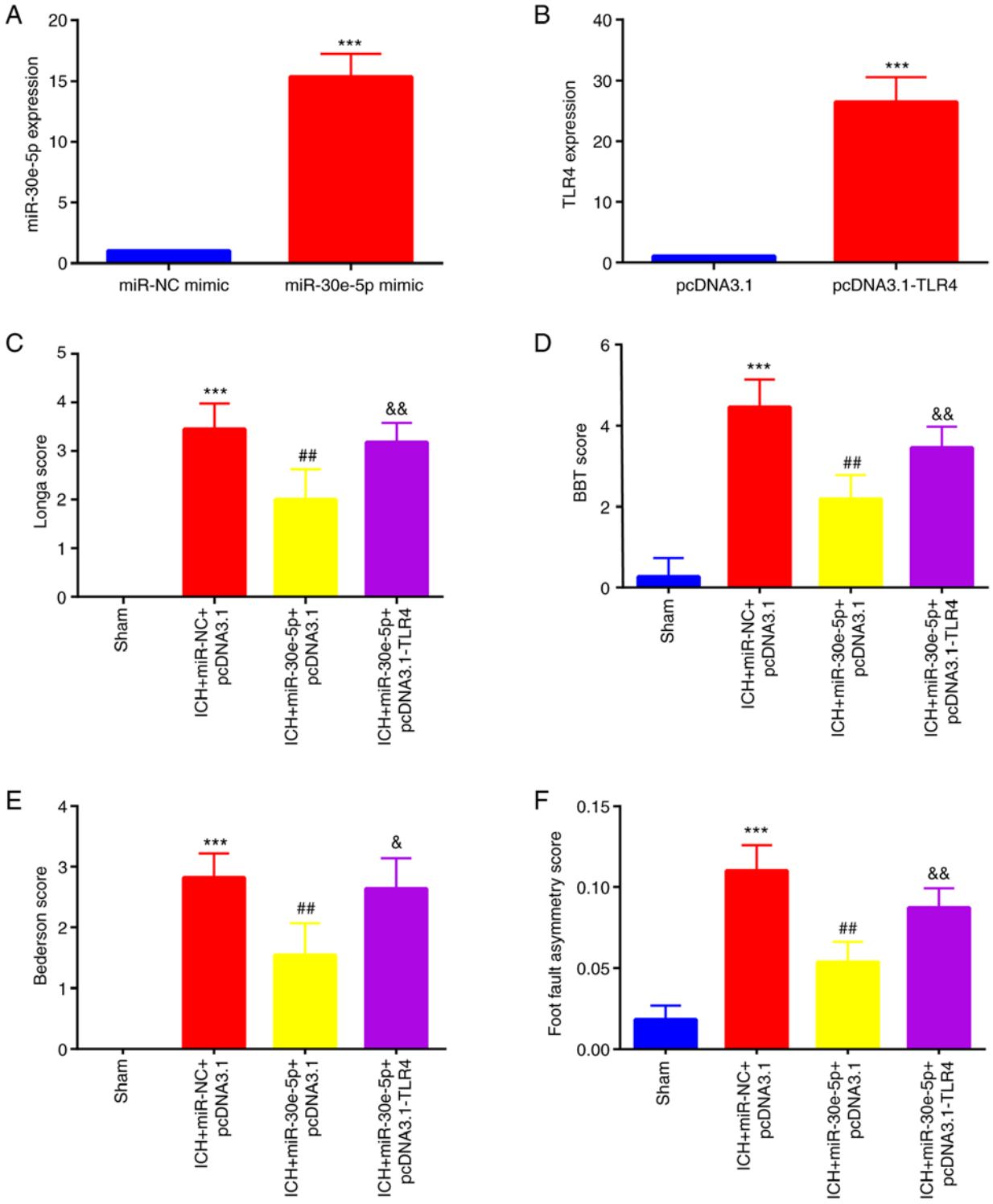

Figure 4. miR-30e-5p attenuates brain injury following ICH by targeting TLR4. Reverse transcription-quantitative PCR was used to detect (A) miR-30e-5p levels in miR-NC and miR-30e-5p mimic (***P<0.001 vs. miR-NC mimic) and (B) TLR4 level in pcDNA3.1 and pcDNA3.1-TLR4 group. n=3. ***P<0.001 vs. pcDNA3.1. A 24-point neurological scoring system was used to test neurological deficit, including (C) Longa, (D) BBT, (E) Bederson and (F) foot fault asymmetry (n=11) in rats in sham, ICH + miR-NC + pcDNA3.1, ICH + miR-30e-5p + pcDNA3.1 and ICH + miR-30e-5p + pcDNA3.1-TLR4 groups. ***P<0.001 vs. sham; $^{\#\#}$P<0.01 vs. ICH + miR-NC + pcDNA3.1; $^{\&}$P<0.01, $^{\&\&}$P<0.01 vs. ICH + miR-30e-5p + pcDNA3.1. ICH, intracerebral hemorrhage; BBT, beam balance test; miR, microRNA; TLR, Toll-like receptor; NC, negative control.

Discussion

ICH is a lethal form of stroke for which there is no effective long-term treatment option (1). As a pathogen recognition receptor (32), TLR4 is involved in regulation of neuroinflammation during ICH (9). However, the role TLR4 in the molecular pathological network of ICH is poorly understood. In the present study, upregulation of TLR4 expression was observed in rats with ICH, which suggested a role for TLR4 in ICH. In addition, miR-30e-5p expression

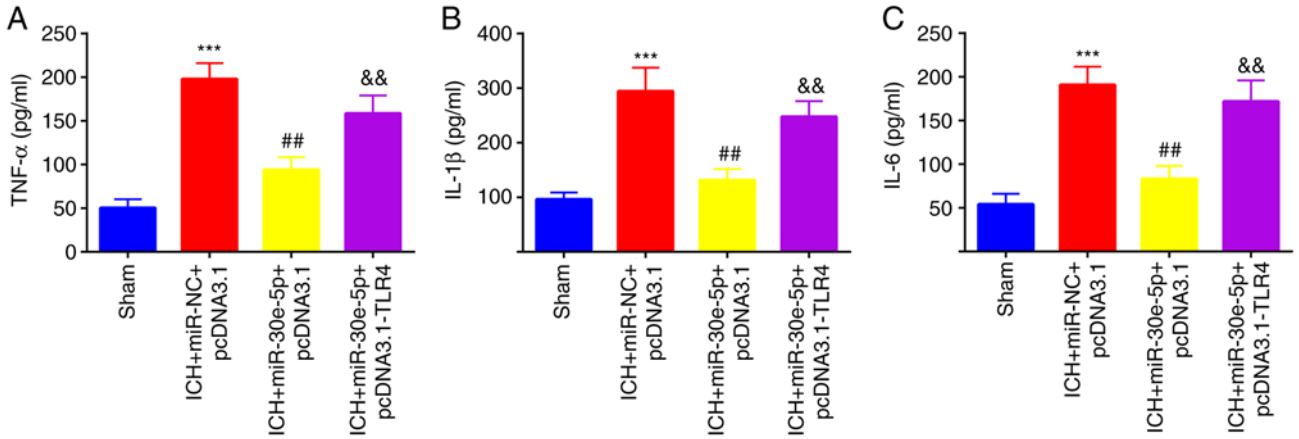

Figure 5. miR-30e-5p overexpression attenuates neuroinflammation by targeting TLR4 following ICH. Proinflammatory cytokines including (A) TNF-α, (B) IL-1β (C) and IL-6 were measured by ELISA in rats in sham, ICH + miR-NC + pcDNA3.1, ICH + miR-30e-5p + pcDNA3.1 and ICH + miR-30e-5p + pcDNA3.1-TLR4 group (n=11). ***P<0.001 vs. sham; ##P<0.01 vs. ICH + miR-NC + pcDNA3.1; &&P<0.01 vs. ICH + miR-30e-5p + pcDNA3.1. ICH, intracerebral hemorrhage; miR, microRNA; TLR, Toll-like receptor; NC, negative control.

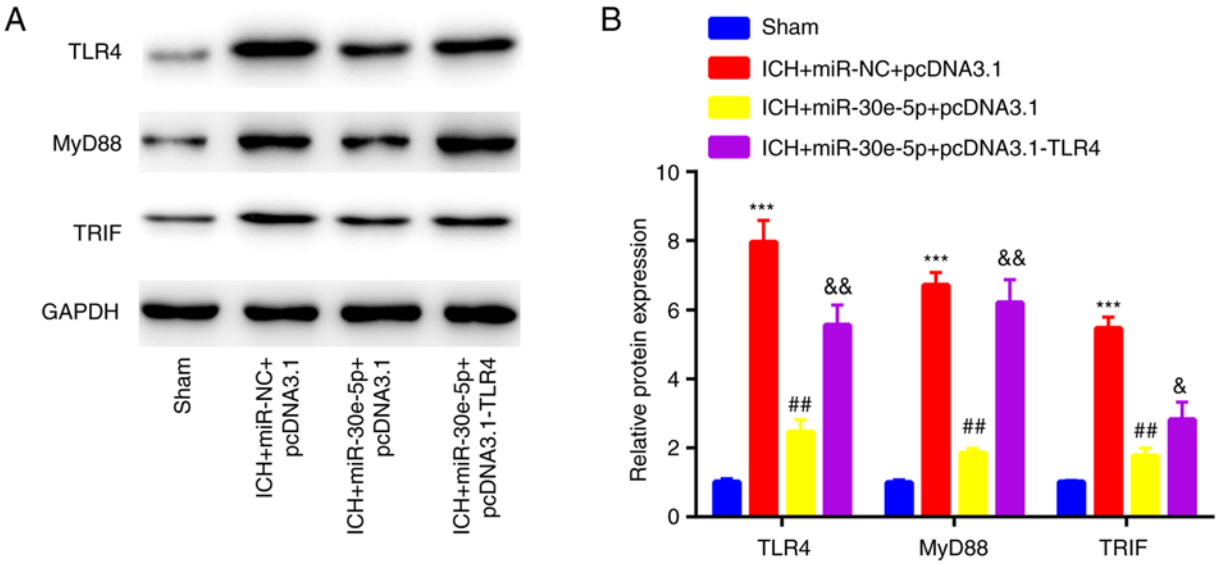

Figure 6. miR-30e-5p overexpression suppresses TLR4 expression and downstream MyD88/TRIF inflammatory signaling pathway following ICH. (A) Western blot analysis was used to detect (B) expression of TLR4, MyD88 and TRIF. n=3. ***P<0.001, vs. sham. ##P<0.01 vs. ICH + miR-NC + pcDNA3.1; &P<0.05, &&P<0.01 vs. ICH + miR-30e-5p + pcDNA3.1. ICH, intracerebral hemorrhage; miR, microRNA; TLR, Toll-like receptor; NC, negative control; MyD88, myeloid differentiation factor 88; TRIF, TIR-domain-containing adapter-inducing interferon-β.

in rats with ICH demonstrated an inverse correlation with TLR4 expression.

miR-30e-5p is associated with a number of diseases (33-35). p53-induced miR-30e-5p expression suppresses metastasis of colorectal cancer by targeting integrin subunit α6 and β1 expression (33). In addition, miR-30e-5p levels are decreased in the plasma of patients with moderate and severe diabetic kidney disease compared with patients with type 1 diabetes mellitus, where miR-30e-5p regulates expression of genes associated with cell apoptosis, differentiation, oxidative stress, angiogenesis and hypoxia (34). In another study, overexpression of miR-30e-5p was found to inhibit endothelial-mesenchymal transition of lipopolysaccharide-treated human brain microvascular endothelial cells by targeting neuronal growth regulator 1 expression (35). However, little is known regarding the association between miR-30e-5p and ICH or the potential interaction between miR-30e-5p and TLR4 in ICH.

ICH induces inflammation to promote edema formation, which triggers detrimental effects in the area surrounding the hematoma, including cell death (7). Increased expression of apoptosis marker cleaved caspase-3 and inflammatory cytokines, including TNF-α, IL-1β and IL-6, has been previously reported in rats with ICH (36). In the present study, miR-30e-5p mimic inhibited TLR4 expression by targeting its 3'UTR. In addition, miR-30e-5p mimic prevented neurological injury, apoptosis and inflammation, as evidenced by rescued neurological deficit score and TNF-α, IL-1β and IL-6 levels in rats with ICH. The neuroprotective effect of miR-30e-5p mimic on rats with ICH was partially reversed by overexpression of TLR4. However, the underlying molecular mechanism of this remains to be elucidated.

It has previously been documented that TLR4 regulates inflammation in ICH by regulating downstream MyD88/TRIF signaling (37). TLR4 interacts with MyD88 and TRIF to regulate gene expression of inflammatory mediators, such as cytokines TNF-α, IL-1β and IL-6 (38,39). The present study also investigated the effects of miR-30e-5p on TLR4/MyD88/TRIF signaling. Overexpression of miR-30e-5p decreased ICH-induced activation of TLR4/MyD88/TRIF signaling. Furthermore, the effect of miR-30e-5p mimic on TLR4/MyD88/TRIF signaling was partially reversed by overexpression of TLR4 in rats with ICH, which demonstrated that the effect of miR-30e-5p mimic on inactivation of TLR4 signaling may be due to its ability to inhibit TLR4 expression. miR-30e-5p decreased luciferase activity of TLR4 construct in PC12 cells. miR-30e-5p was inversely correlated with TLR4 expression and miR-30e-5p overexpression decreased TLR4 expression in rat brain following ICH.

PiggyBac, which is frequently used for gene overexpression, can be inserted into genome to make overexpression more durable (40); PiggyBac should be used in future study to improve the stability of miR-30e-5p overexpression. Additionally, the present study focused on changes in behavioral performance; pathological images of brain and neurons in sham and ICH groups will be obtained by another ongoing study.

Collectively, the present results indicated that miR-30e-5p overexpression decreased TLR4 expression in the brain tissue of rats with ICH, resulting in inactivation of MyD88/TRIF signaling and protection against neurological deficit, apoptosis and inflammation. The present study provided mechanistic insight into how miR-30e-5p exerts neurological protection in rats with ICH.

Acknowledgements

Not applicable.

Funding

No funding was received.

Availability of data and materials

The datasets used and/or analyzed during the current study are available from the corresponding author on reasonable request.

Authors' contributions

HS and NX performed experiments and data analysis. SJ designed and supervised the study and wrote and revised the manuscript. All authors have read and approved the final manuscript. HS and SJ confirm the authenticity of all the raw data.

Ethics approval and consent to participate

The animal experiments were approved by the Institutional Animal Care and Use Committee of Jinan First People's Hospital (approval no. JNFPH2019-03; Ji'nan, China).

Patient consent for publication

Not applicable.

Competing interests

The authors declare that they have no competing interests.

References

1. Xi G, Strahle J, Hua Y and Keep RF: Progress in translational research on intracerebral hemorrhage: Is there an end in sight? Prog Neurobiol 115: 45-63, 2014.
2. Ziai WC and Carhuapoma JR: Intracerebral hemorrhage. Continuum (Minneap Minn) 24: 1603-1622, 2018.
3. van Asch CJ, Luitse MJ, Rinkel GJ, van der Tweel I, Algra A and Klijn CJ: Incidence, case fatality, and functional outcome of intracerebral haemorrhage over time, according to age, sex, and ethnic origin: A systematic review and meta-analysis. Lancet Neurol 9: 167-176, 2010.
4. Qureshi AI, Tuhrim S, Broderick JP, Batjer HH, Hondo H and Hanley DF: Spontaneous intracerebral hemorrhage. N Engl J Med 344: 1450-1460, 2001.
5. Rymer MM: Hemorrhagic stroke: Intracerebral hemorrhage. Mo Med 108: 50-54, 2011.
6. Rodríguez JA, Sobrino T, López-Arias E, Ugarte A, Sánchez-Arias JA, Vieites-Prado A, de Miguel I, Oyarzabal J, Páramo JA, Campos F, *et al*: cM352 reduces brain damage and improves functional recovery in a rat model of intracerebral hemorrhage. J Am Heart Assoc 6: e006042, 2017.
7. Sheth KN and Rosand J: Targeting the immune system in intracerebral hemorrhage. JAMA Neurol 71: 1083-1084, 2014.
8. Zhou Y, Wang Y, Wang J, Anne Stetler R and Yang QW: Inflammation in intracerebral hemorrhage: From mechanisms to clinical translation. Prog Neurobiol 115: 25-44, 2014.
9. Rivest S: Regulation of innate immune responses in the brain. Nat Rev Immunol 9: 429-439, 2009.
10. Fang H, Wang PF, Zhou Y, Wang YC and Yang QW: Toll-like receptor 4 signaling in intracerebral hemorrhage-induced inflammation and injury. J Neuroinflammation 10: 27, 2013.
11. Zhang D, Shen X, Pang K, Yang Z and Yu A: VSIG4 alleviates intracerebral hemorrhage induced brain injury by suppressing TLR4-regulated inflammatory response. Brain Res Bull 176: 67-75, 2021.
12. Sansing LH, Harris TH, Welsh FA, Kasner SE, Hunter CA and Kariko K: Toll-like receptor 4 contributes to poor outcome after intracerebral hemorrhage. Annal Neurol 70: 646-656, 2011.
13. Wang YC, Wang PF, Fang H, Chen J, Xiong XY and Yang QW: Toll-like receptor 4 antagonist attenuates intracerebral hemorrhage-induced brain injury. Stroke 44: 2545-2552, 2013.
14. Ambros V: The functions of animal microRNAs. Nature 431: 350-355, 2004.
15. Liu DZ, Tian Y, Ander BP, Xu H, Stamova BS, Zhan X, Turner RJ, Jickling G and Sharp FR: Brain and blood microRNA expression profiling of ischemic stroke, intracerebral hemorrhage, and kainate seizures. J Cereb Blood Flow Metab 30: 92-101, 2010.
16. Wang Y, Song Y, Pang Y, Yu Z, Hua W, Gu Y, Qi J and Wu H: miR-183-5p alleviates early injury after intracerebral hemorrhage by inhibiting heme oxygenase-1 expression. Aging (Albany NY) 12: 12869-12895, 2020.
17. Nie H, Hu Y, Guo W, Wang W, Yang Q, Dong Q, Tang Y, Li Q and Tang Z: miR-331-3p inhibits inflammatory response after intracerebral hemorrhage by directly targeting NLRP6. Biomed Res Int 2020: 6182464, 2020.
18. Wang J, Zhu Y, Jin F, Tang L, He Z and He Z: Differential expression of circulating microRNAs in blood and haematoma samples from patients with intracerebral haemorrhage. J Int Med Res 44: 419-432, 2016.
19. Zhang S, Li G, Liu C, Lu S, Jing Q, Chen X, Zheng H, Ma H, Zhang D, Ren S, *et al*: miR-30e-5p represses angiogenesis and metastasis by directly targeting AEG-1 in squamous cell carcinoma of the head and neck. Cancer Sci 111: 356-368, 2020.
20. Zhang Z, Qin H, Jiang B, Chen W, Cao W, Zhao X, Yuan H, Qi W, Zhuo D and Guo H: miR-30e-5p suppresses cell proliferation and migration in bladder cancer through regulating metadherin. J Cell Biochem 120: 15924-15932, 2019.

21. Mo B, Wu X, Wang X, Xie J, Ye Z and Li L: miR-30e-5p mitigates hypoxia-induced apoptosis in human stem cell-derived cardiomyocytes by suppressing Bim. Int J Biol Sci 15: 1042-1051, 2019.
22. Chen Y, Yin Y and Jiang H: miR-30e-5p alleviates inflammation and cardiac dysfunction after myocardial infarction through targeting PTEN. Inflammation 44: 769-779, 2021.
23. Li W, Li X, Li T, Jiang MG, Wan H, Luo GZ, Feng C, Cui X, Teng F, Yuan Y, *et al*: Genetic modification and screening in rat using haploid embryonic stem cells. Cell Stem Cell 14: 404-414, 2014.
24. Li T, Shuai L, Mao J, Wang X, Wang M, Zhang X, Wang L, Li Y, Li W and Zhou Q: Efficient production of fluorescent transgenic rats using the piggyBac Transposon. Sci Rep 6: 33225, 2016.
25. Jung KH, Chu K, Jeong SW, Han SY, Lee ST, Kim JY, Kim M and Roh JK: HMG-CoA reductase inhibitor, atorvastatin, promotes sensorimotor recovery, suppressing acute inflammatory reaction after experimental intracerebral hemorrhage. Stroke 35: 1744-1749, 2004.
26. Ge XT, Lei P, Wang HC, Zhang AL, Han ZL, Chen X, Li SH, Jiang RC, Kang CS, and Zhang JN: miR-21 improves the neurological outcome after traumatic brain injury in rats. Sci Rep 4: 6718, 2014.
27. Bachour SP, Hevesi M, Bachour O, Sweis BM, Mahmoudi J, Brekke JA and Divani AA: Comparisons between Garcia, Modo, and Longa rodent stroke scales: Optimizing resource allocation in rat models of focal middle cerebral artery occlusion. J Neurol Sci 364: 136-140, 2016.
28. Yue X, Liu L, Yan H, Gui Y, Zhao J and Zhang P: Intracerebral hemorrhage induced brain injury is mediated by the interleukin-12 receptor in rats. Neuropsychiatr Dis Treat 16: 891-900, 2020.
29. Liu H, Shen H, Harvey BK, Castillo P, Lu H, Yang Y and Wang Y: Post-treatment with amphetamine enhances reinnervation of the ipsilateral side cortex in stroke rats. NeuroImage 56: 280-289, 2011.
30. Han J, Zhang J, Zhong Z, Li Z, Pang W, Hu J and Chen L: Gualou Guizhi decoction promotes neurological functional recovery and neurogenesis following focal cerebral ischemia/reperfusion. Neural Regen Res 13: 1408-1416, 2018.
31. Livak KJ and Schmittgen TD: Analysis of relative gene expression data using real-time quantitative PCR and the 2(-Delta Delta C(T)) method. Methods 25: 402-408, 2001.
32. Molteni M, Gemma S and Rossetti C: The role of toll-like receptor 4 in infectious and noninfectious inflammation. Mediators Inflamm 2016: 6978936, 2016.
33. Laudato S, Patil N, Abba ML, Leupold JH, Benner A, Gaiser T, Marx A and Allgayer H: P53-induced miR-30e-5p inhibits colorectal cancer invasion and metastasis by targeting ITGA6 and ITGB1. Int J Cancer 141: 1879-1890, 2017.
34. Dieter C, Assmann TS, Costa AR, Canani LH, de Souza BM, Bauer AC and Crispim D: MiR-30e-5p and MiR-15a-5p expressions in plasma and urine of type 1 diabetic patients with diabetic kidney disease. Front Genet 10: 563, 2019.
35. Dong Y, Fan X, Wang Z, Zhang L and Guo S: Circ_HECW2 functions as a miR-30e-5p sponge to regulate LPS-induced endothelial-mesenchymal transition by mediating NEGR1 expression. Brain Res 1748: 147114, 2020.
36. Wang SD, Cui YJ, Xu JQ and Gao H: miR-140-5p attenuates neuroinflammation and brain injury in rats following intracerebral hemorrhage by targeting TLR4. Inflammation 42: 1869-1877, 2019.
37. Lin S, Yin Q, Zhong Q, Lv FL, Zhou Y, Li JQ, Wang JZ, Su BY and Yang QW: Heme activates TLR4-mediated inflammatory injury via MyD88/TRIF signaling pathway in intracerebral hemorrhage. J Neuroinflamm 9: 46, 2012.
38. Miyake K: Endotoxin recognition molecules MD-2 and toll-like receptor 4 as potential targets for therapeutic intervention of endotoxin shock. Curr Drug Targets Inflamm Allergy 3: 291-297, 2004.
39. Takeda K and Akira S: TLR signaling pathways. Semin Immunol 16: 3-9, 2004.
40. Zhang W, Tian Y, Gao Q, Li X, Li Y, Zhang J, Yao C, Wang Y, Wang H, Zhao Y, *et al*: Inhibition of apoptosis reduces diploidization of haploid mouse embryonic stem cells during differentiation. Stem Cell Reports 15: 185-197, 2020.

This work is licensed under a Creative Commons Attribution-NonCommercial-NoDerivatives 4.0 International (CC BY-NC-ND 4.0) License.